Nucleotide Regulation of *Escherichia coli* Glycerol Kinase: Initial-Velocity and Substrate Binding Studies†

Donald W. Pettigrew,* Gui-Ju Yu,‡ and Youguo Liu‡,§

Department of Biochemistry and Biophysics, Texas A&M University, College Station, Texas 77843-2128

Received March 27, 1990; Revised Manuscript Received June 22, 1990

ABSTRACT: Substrate binding to *Escherichia coli* glycerol kinase (EC 2.7.1.30; ATP:glycerol 3-phosphotransferase) was investigated by using both kinetics and binding methods. Initial-velocity studies in both reaction directions show a sequential kinetic mechanism with apparent substrate activation by ATP and substrate inhibition by ADP. In addition, the Michaelis constants differ greatly from the subtrate dissociation constants. Results of product inhibition studies and dead-end inhibition studies using 5′-adenylyl imidodiphosphate show the enzyme has a random kinetic mechanism, which is consistent with the observed formation of binary complexes with all the substrates and the glycerol-independent MgATPase activity of the enzyme. Dissociation constants for substrate binding determined by using ligand protection from inactivation by *N*-ethylmaleimide agree with those estimated from the initial-velocity studies. Determinations of substrate binding stoichiometry by equilibrium dialysis show half-of-the-sites binding for ATP, ADP, and glycerol. Thus, the regulation by nucleotides does not appear to reflect binding at a separate regulatory site. The random kinetic mechanism obviates the need to postulate such a site to explain the formation of binary complexes with the nucleotides. The observed stoichiometry is consistent with a model for the nucleotide regulatory behavior in which the dimer is the enzyme form present in the assay and its subunits display different substrate binding affinities. Several properties of the enzyme are consistent with negative cooperativity as the basis for the difference in affinities. The possible physiological importance of the regulatory behavior with respect to ATP is considered.

Glycerol kinase (EC 2.7.1.30; ATP:glycerol 3-phosphotransferase) catalyzes the MgATP-dependent phosphorylation of glycerol to yield glycerol-3P (Lin, 1976).[1] In *Escherichia coli*, the role of this enzyme is mobilization of glycerol to serve as a carbon source. The glycerol-3P is subsequently oxidized to dihydroxyacetone phosphate and enters glycolysis/gluconeogenesis. Glycerol-3P also serves as the inducer for the *glp* regulon, one member of which is the *glpK* gene, which codes for glycerol kinase and has been cloned and sequenced (Pettigrew et al., 1988).

Glycerol kinase catalyzes the rate-limiting step in glycerol utilization by *E. coli* (Zwaig et al., 1970) and is a regulatory enzyme whose activity is modulated by several effectors. Its activity is inhibited by the glycolytic intermediate fructose 1,6-bisphosphate (Zwaig & Lin, 1966) and by protein–protein interactions with enzyme III^{glc} of the phosphotransferase system (Novotny et al., 1985). At pH 7.0, the steady-state kinetics display regulatory behavior with respect to ATP (Thorner & Paulus, 1973; Pettigrew, 1986).[2] The double-reciprocal plots with respect to ATP are concave downward, indicating either negative homotropic interactions or two classes of ATP binding sites.

The apparent activation by ATP is paradoxical behavior for an enzyme at the start of a catabolic pathway that will yield ATP.[3] Another apparent paradox in the behavior of this enzyme is the formation of high-affinity binary complexes with nucleotides (Pettigrew, 1986, 1987) because the kinetic mechanism is reportedly ordered, with glycerol binding before ATP (Thorner & Paulus, 1973). The formation of the binary complexes suggests the presence of regulatory binding sites for nucleotides, which may account for the nucleotide regulation. The nucleotide binding sites were investigated by using affinity labeling, which inactivated the enzyme and modified it to the extent of 1 site/subunit but did not resolve the apparent paradoxes (Pettigrew, 1987). This report describes initial-velocity and substrate binding studies, which show the enzyme displays half-of-the-sites binding toward its substrates and has a random kinetic mechanism. These results explain the formation of binary complexes with nucleotides and provide a possible explanation for the nucleotide regulation.

Materials and Methods

Materials. All chemicals and enzymes were purchased from Sigma Chemical Co. and used without further purification, unless otherwise indicated. Tritium-labeled substrates were purchased from New England Nuclear. NEM was a product of Pierce Chemical Co.

Glycerol kinase was purified from *E. coli* carrying the *glpK* gene on a high-expression plasmid (Faber et al., 1989) and stored as a crystalline ammonium sulfate suspension as previously described (Pettigrew, 1986). For use in experiments, the crystals were dissolved in 0.1 M triethanolamine hydro-

† Supported by a grant from the Robert A. Welch Foundation (A-1061) and by the Texas Agricultural Experiment Station (H-6559).

* To whom correspondence should be addressed.

‡ Postdoctoral fellow of the Robert A. Welch Foundation.

§ Permanent address: Department of Nucleic Acids of the Institute of Biophysics, Chinese Academy of Science, Beijing, China. Deceased November 9, 1988.

[1] Abbrevations: AMP-PNP, adenylyl imidodiphosphate; glycerol-3P, *sn*-glycerol 3-phosphate; NEM, *N*-ethylmaleimide.

[2] In most of the experiments, Mg^{2+} is present at a total concentration of 10 mM because it is required for catalytic activity; thus, there is little free nucleotide present. However, in describing the experiments, only the total nucleotide concentration is considered. The enzyme is not inhibited by free Mg^{2+} at these concentrations.

[3] Because the apparent maximum velocity increases, the effects of ATP will be characterized as substrate activation, despite the increase in the apparent Michaelis constant, i.e., decrease in apparent affinity for ATP.

0006-2960/90/0429-8620$02.50/0 © 1990 American Chemical Society

chloride buffer at pH 7 and separated from the remaining components of the crystallization buffer by dialysis or by chromatography on Sephadex G-25. The concentration of the enzyme was determined from the absorbance at 280 nm by using an extinction coefficient of 1.4 $(mg/mL)^{-1}$ cm^{-1} (Thorner & Paulus, 1971) or 78.65 mM^{-1} (subunit) cm^{-1}, based on a subunit molecular weight of 56 100 daltons (Pettigrew et al., 1988). For equilibrium dialysis, crystalline enzyme was dissolved in minimal 0.1 M triethanolamine hydrochloride buffer at pH 7 and exhaustively dialyzed versus the same buffer at 4 °C. For some experiments, the enzyme was further concentrated by using an Amicon Centricon concentrator.

Initial Velocity Studies. Initial velocities were measured by using a Beckman DU-6 spectrophotometer equipped with a kinetics software package. In all experiments, the cuvette contained 50 mM triethanolamine hydrochloride buffer, pH 7, 10 mM $MgCl_2$, and 20 mM KCl, with substrates and other ligands at the concentrations indicated in the figure legends and table. The temperature was maintained at 25 °C with a refrigerated circulating water bath. After thermal equilibration of the cuvettes, the reactions were initiated by addition of glycerol kinase to the concentrations given in the figure legends and table. For the forward reaction direction, velocities were determined by using an ADP-coupled assay (Pettigrew, 1986) with 40 units of pyruvate kinase, 100 units of lactate dehydrogenase, and 0.2 mM each NADH and phosphoenolpyruvate. In the reverse direction, velocities were determined by using an ATP-coupled assay with 12.5 μg of hexokinase, 6.25 μg of glucose 6-phosphate dehydrogenase, 2 mM glucose, and 0.3 mM $NADP^+$, and the blank rate was subtracted from the observed rate for all assays. Each *point* shown in the figures is the average of duplicate or triplicate determinations.

The initial-velocity data were analyzed by using a nonlinear least-squares computer program (Turner et al., 1981) to fit the data to eqs 1–4. Equation 2 was used to fit initial-velocity

$$v = VAB/K_{ia}K_b + K_aB + K_bA + AB) \quad (1)$$

$$v = V_1AB/(K_{ia1}K_{b1} + K_{a1}B + K_{b1}A + AB) + V_2AB/(K_{ia2}K_{b2} + K_{a2}B + K_{b2}A + AB) \quad (2)$$

$$v = VA/[K(1 + I/K_{is}) + A(1 + I/K_{ii})] \quad (3)$$

$$v = VA/[K(1 + I/K_{is}) + A] \quad (4)$$

data obtained as a function of ATP concentration. The fits were accomplished in a stepwise fashion. First, data at the lower ATP concentrations were fitted by using eq 1. The parameter values obtained were then used as the subscripted 1 parameters in fits to eq 2, with their values held fixed. Equations 3 and 4 were used to fit data for noncompetitive and competitive inhibition, respectively.

Ligand Binding Studies. Affinities for substrate binding were determined from the ligand concentration dependence of the rate of inactivation of the enzyme by NEM. The incubations at pH 7 and 25 °C were done as previously described (Pettigrew, 1986), by using 5 mM NEM to initiate the inactivation reactions, with ligands added to the incubation as indicated in the figures and table. The pseudo-first-order rate constants, k, for the inactivation were obtained from nonlinear least-squares fits (Turner et al., 1981) of the inactivation data to the equation

$$(SA)_t = (SA)_0e^{-kt} \quad (5)$$

where $(SA)_t$ is the specific activity at time t and $(SA)_0$ is the specific activity at time zero, i.e., the amplitude. The dissociation constant for ligand binding, K_L, was estimated by fitting the ligand concentration, L, dependence of the apparent rate constant, k_{app}, to the equation

$$k_{app} = (k_e + k_{el}L/K_L)/(1 + L/K_L) \quad (6)$$

where k_e is the rate constant for inactivation of the enzyme alone and k_{el} is the rate constant for inactivation of the enzyme/ligand complex. This equation describes the inactivation kinetics for cases in which the ligand does not provide complete protection from inactivation but does alter the rate of the inactivation, and it was derived following the treatment of Scrutton and Utter (1965).

Stoichiometries of ligand binding were determined by using a 100-mL Dia-Cell equilibrium dialysis apparatus (InstruMed, Inc., Union Bridge, MD) with 9-mm dialysis capsules. Dialysis tubing (Spectrum) was heated to boiling once in 1 mM EDTA at pH 7 and twice in distilled water and stored in 50% ethanol at 4 °C. To assemble the apparatus, a disk of rinsed dialysis tubing was cut with a cork borer. After the disk was assembled in the apparatus according to the manufacturer's instructions, it was seized with unwaxed dental floss with a clove hitch and two half-hitches to prevent leaks. Water was added to test for leaks, and the tested apparatus was filled with buffer (0.1 M triethanolamine hydrochloride and 0.1 mM EDTA, pH 7.0) to rinse the dialysis tubing. After the buffer was removed, a solution of the desired ligand in the same buffer was added to the lower part of the apparatus, which contained a magnetic stir bar. Glycerol kinase at a concentration of 25–58 mg/mL in a volume of 150–200 μL was placed into the upper compartment of the apparatus, which also contained a small magnetic stir bar. The apparatus was placed on a magnetic stir plate on a rocker table, with a styrofoam insulator between the apparatus and the stir plate to prevent heating. The dialysis solutions were mixed by rocking and stirring at room temperature. Dialyses were performed for 10–12 h; control experiments without enzyme showed the ligand concentrations in the lower and upper compartments reached equilibrium in 6–8 h. After dialysis, the solutions were removed from both compartments, and aliquots were analyzed for protein concentration, ligand concentration, and glycerol kinase activity. The concentrations of protein and nucleotides were determined from measurements of absorbances at 259 and 280 nm, by solving simultaneous equations and using the following extinction coefficients (cm^{-1}): at 280 nm, 78.65 mM^{-1} for glycerol kinase and 2.31 mM^{-1} for ATP and ADP; at 259 nm, 40 mM^{-1} for glycerol kinase and 15.4 mM^{-1} for ATP and ADP. The concentrations of glycerol in the solutions after dialysis were determined by using [^{3}H]glycerol and scintillation counting. The specific radioactivity of the glycerol was determined by counting a known concentration of radioactive glycerol under identical conditions; control experiments showed neither the protein nor incubation of the radioactive glycerol in the dialysis apparatus affected the counting efficiency. For determinations of the specific radioactivity, the concentration of glycerol was determined by using glycerol kinase in the ADP-coupled assay. The activity of glycerol kinase was determined by using the ADP-coupled assay; the activity never changed by more than 5% over the course of the dialysis. Thus, the enzyme is quite stable under these conditions.

The nucleotide solutions from the lower compartment of the apparatus were analyzed by reverse-phase HPLC to evaluate hydrolysis of the nucleotides. Analysis of the elution profiles by both absorbance at 254 nm and scintillation counting using ^{3}H-labeled nucleotides showed less than 1% hydrolysis of either ADP or ATP during the course of the experiments.

The ability of the equilibrium dialysis method to detect multiple ATP binding sites per subunit was tested by using phosphoglycerate kinase and repeating the experiment de-

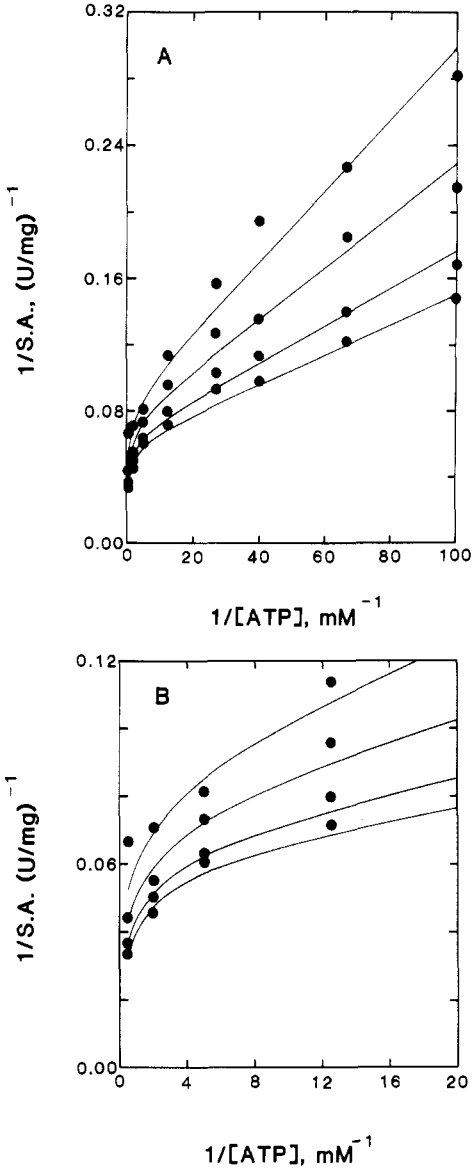

FIGURE 1: ATP dependence of the initial velocity in the forward reaction direction. The *points* are the experimental data, and the *lines* are the fit to eq 2 with the parameters shown in Table I. Glycerol concentrations, mM: 0.015, 0.025, 0.05, and 0.1. Glycerol kinase concentration: 0.18 μg/mL. Panel A shows the entire range of ATP concentrations, and panel B shows only the higher ATP concentrations.

scribed by Scopes (1978). The stoichiometry of MgATP binding was determined at 4 °C by using equilibrium dialysis as described above with 1.05 mM phosphoglycerate kinase and 5.1 mM ATP in the buffer described by Scopes (1978). After dialysis, the concentrations of phosphoglycerate kinase and ATP were determined from absorbance measurements at 259 and 280 nm, with the extinction coefficients given by Scopes (1978).

RESULTS

Initial Velocity Studies. Initial-velocity studies were performed for both reaction directions. The dependence of the initial velocity on nucleotide concentration is shown as double-reciprocal plots in Figures 1 and 2. In the forward reaction (Figure 1), apparent substrate activation by ATP is observed, in agreement with previous reports (Thorner & Paulus, 1973; Pettigrew, 1986). In the reverse reaction (Figure 2), apparent excess substrate inhibition by ADP is observed, which has not been previously reported. Thus, both reaction directions show nonlinear double-reciprocal plots.

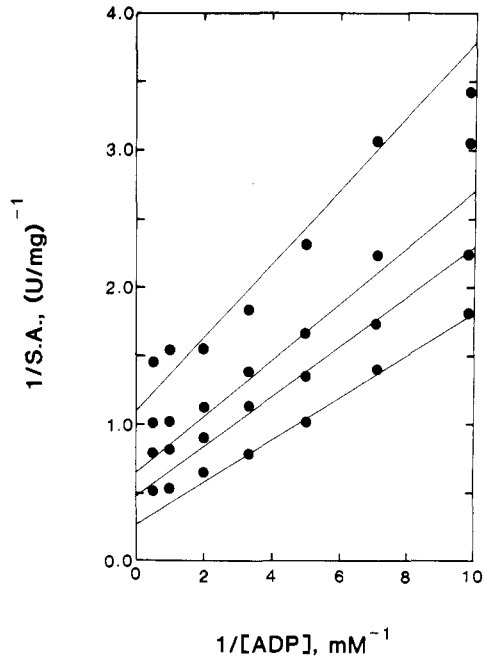

FIGURE 2: ADP dependence of the initial velocity in the reverse reaction direction. The *points* are the experimental data, and the *lines* are the fit of data obtained at ADP concentrations less than 0.3 mM to eq 1 with the parameter values shown in Table I. Glycerol-3P concentrations, mM: 0.05, 0.1, 0.16, and 0.57. Glycerol kinase concentration: 1.5 μg/mL.

Although the overall double-reciprocal plots are nonlinear, the data at the lower nucleotide concentrations are linear for both reaction directions and are well described by a sequential kinetic mechanism. In the forward reaction direction, the data were fitted to eq 2 as described under Materials and Methods. The *lines* in Figure 1 show that this provides a good description of the data. Equation 2 describes the data in terms of a sequential kinetic mechanism with two classes of noninteracting ATP binding sites; other possible cases are considered below. For the reverse reaction, the data at ADP concentrations of less than 0.3 mM were fitted to eq 1; i.e., data at higher ADP concentrations were omitted from the fit. The *lines* in figure 2 show that eq 1 provides a good description of the data at the lower nucleotide concentrations. The agreement between the dissociation constants obtained from these fits of the initial-velocity data and those obtained independently from substrate binding studies described below validates this treatment of the initial-velocity data.

Initial-velocity constants obtained from the fits are summarized in Table I. The substrate Michaelis constants differ from the dissociation constants for both reaction directions. In the forward reaction, the Michaelis constants are 10-fold less than the dissociation constants for the apparent higher affinity ATP binding site. The converse is observed for the reverse reaction and for the apparent lower affinity ATP site in that the Michaelis constants are 7-fold and 5-fold greater, respectively, than the dissociation constants. The maximum velocities in each reaction direction are different. The V_{max} for the apparent higher affinity ATP site and the total V_{max} for the forward reaction are 3-fold and 7-fold greater, respectively, than those of the reverse reaction.

The difference in the kinetic properties of the two apparent classes of ATP site is striking. For the lower affinity site, V_{max} is 2-fold greater, the K_m for glycerol is 5-fold greater, and the K_m for ATP is 307-fold greater than the values obtained for the higher affinity site. The relations between the Michaelis and dissociation constants are also different: for the higher

Table I: Kinetic Constants and Substrate Binding[a]

substrate A	substrate B	K_a (μM)	K_{ia} (μM)	K_b (μM)	V_{max} (units/mg)	k_{cat}/K_{ma} (M^{-1} s^{-1})	k_{cat}/K_{mb} (M^{-1} s^{-1})
		Initial-Velocity Constants					
ATP	glycerol	8.4 ± 0.7	86 ± 25	4.9 ± 1.2	15.7 ± 0.3	(1.7 ± 0.17) × 10^6	(3 ± 0.8) × 10^6
ATP[b]	glycerol	2580 ± 1130	230 ± 490	26 ± 10	36.9 ± 10.8		
ADP	glycerol-3P	770 ± 220	140 ± 70	240 ± 100	5.3 ± 1.3	(6.5 ± 3.4) × 10^3	(2 ± 1.3) × 10^4

inhibitor	variable substrate	fixed substrate [concn (mM)]	$K_{is,app}$ (mM)	$K_{ii,app}$ (mM)	type of inhibition	$K_{is,true}$ (mM)	$K_{ii,true}$ (mM)
		Product and Dead-End Inhibition Constants					
glycerol-3P	glycerol	ATP [0.05]	0.20 ± 0.04		C	0.13 ± 0.4	
glycerol-3P	ATP	glycerol [0.05]	0.28 ± 0.03		C	0.14 ± 0.6	
glycerol	ADP	glycerol-3P [0.57]	0.32 ± 0.13	0.053 ± 0.007	NC	0.023 ± 0.02	0.016 ± 0.007
AMP-PNP	glycerol	ATP [0.05]	3.7 ± 1.2	4.2 ± 0.5	NC	2.3 ± 1.0	0.60 ± 0.11
AMP-PNP	ATP	glycerol [1.1]	0.57 ± 0.08		C	*c*	
AMP-PNP	glycerol-3P	ADP [1.0]	2.7 ± 1.0	2.5 ± 0.4	NC	0.33 ± 0.27	0.48 ± 0.35
AMP-PNP	ADP	glycerol-3P [0.5]	0.49 ± 0.09		C	*c*	

ligand	K_L (mM) no Mg^{2+}	K_L (mM) 10 mM $MgCl_2$	K_{iL} (mM)	stoichiometry[d]
	Substrate Binding			
ADP	0.12 ± 0.02	0.15 ± 0.04	0.14 ± 0.07	0.38 ± 0.13 (5)
ATP	0.11 ± 0.02	0.067 ± 0.011	0.086 ± 0.025	0.58 ± 0.21 (9)
AMP-PNP	0.20 ± 0.04	0.20 ± 0.03		nd
glycerol	0.047 ± 0.018	nd	0.050 ± 0.032	0.59 ± 0.08 (8)
glycerol-3P	0.087 ± 0.012	0.057 ± 0.012	0.044 ± 0.022	nd

[a] The expressed uncertainties are the confidence limits obtained from fitting the data to the appropriate equations, except for stoichiometry, for which the standard deviation is given. nd, not determined. [b] Fit to the higher concentrations of ATP by using eq 2. See text. [c] Since the concentration of nonvaried substrate approaches saturation, $K_{is,app}$ gives the true dissociation constant for binding to E/nonvaried substrate binary complex. See text. [d] Mol of ligand bound/mol of glycerol kinase subunit. The number of determinations is given in parentheses.

affinity site, the Michaelis constants are less than the dissociation constants, while the converse is true for the lower affinity site. The 2-fold difference in the apparent V_{max} is interesting and suggests the turnover numbers of the two types of site are the same.

Product and Dead-End Inhibition Studies. Product inhibition studies were performed in both reaction directions. Linear double-reciprocal plots were obtained in all cases (not show), and the data were analyzed by fitting to eq 3 or eq 4. Results of these studies are summarized in Table I.

The product inhibition studies are consistent with a random kinetic mechanism in which the enzyme/glycerol-3P/MgATP dead-end complex does not form. Glycerol-3P is a competitive inhibitor versus both glycerol and ATP. The competitive inhibition with respect to glycerol is expected from the structural similarity of these substrates. The value of $K_{is,true}$ obtained for binding of glycerol-3P to the free enzyme agrees well with the value of $K_{iglycerol\text{-}3P}$ obtained from the initial-velocity studies. Glycerol is a noncompetitive inhibitor with respect to ADP, indicating that the enzyme/glycerol/MgADP dead-end complex does form. The value of $K_{is,true}$ obtained for binding of glycerol to the free enzyme agrees well with the value of $K_{iglycerol}$ obtained from the initial-velocity studies. The agreement between the values of $K_{is,true}$ and $K_{ii,true}$ suggests the absence of interactions in the binding of glycerol and ADP to form the ternary complex.

The dead-end inhibition studies are also consistent with a random kinetic mechanism. No uncompetitive patterns were observed. AMP-PNP is a competitive inhibitor with respect to both ATP and ADP and is a noncompetitive inhibitor with respect to both glycerol and glycerol-3P. The competitive inhibition versus ATP or ADP is expected because of the structural similarity between these ligands. Because of the high concentration of nonvaried substrate used, $K_{is,app}$ for competitive inhibition versus ATP or ADP gives the dissociation constant for binding of AMP-PNP to the enzyme/glycerol and enzyme/glycerol-3P complexes, respectively. The agreement between these values indicates no difference in affinity of these complexes for AMP-PNP. This indicates differences in the binding of ATP and AMP-PNP, showing that AMP-PNP forms a ternary complex with enzyme/glycerol-3P while ATP does not. In the case of the noncompetitive inhibition versus glycerol-3P, $K_{is,true}$ agrees with the value for the dissociation constant for AMP-PNP binding to the free enzyme, K_L (Table I), as determined independently by using protection from inactivation by NEM (see below). The value of $K_{ii,true}$ agrees with the dissociation constant for binding of AMP-PNP to the enzyme/glycerol-3P complex determined from the competitive inhibition of AMP-PNP versus ADP. In the case of the noncompetitive inhibition of AMP-PNP versus glycerol, the $K_{ii,true}$ agrees with the dissociation constant for binding of AMP-PNP to the enzyme/glycerol complex determined from competitive inhibition of AMP-PNP versus ATP. However, the value of $K_{is,true}$ is 10-fold greater than the value estimated from noncompetitive inhibition versus glycerol-3P. This suggests that the term used to correct $K_{is,app}$, $[1/(1 + [ATP]/K_{iATP})]$, does not provide sufficient correction. This may indicate that rate constants for processes other than the binding and dissociation of AMP-PNP from the free enzyme should be included but are not.

Results of both the product and dead-end inhibition studies are consistent with a random kinetic mechanism. Thus, either substrate in either reaction direction can form a binary complex with the enzyme. This conclusion is consistent with the formation of binary complexes with all substrates, as observed in chemical modification studies (Pettigrew, 1986, 1987).

MgATPase Activity. A random kinetic mechanism for *E. coli* glycerol kinase is further supported by the observation of a glycerol-independent MgATPase activity. Initial-velocity studies at an enzyme concentration of 1 mg/mL show the enzyme catalyzes the glycerol-independent hydrolysis of ATP to ADP. The apparent K_m for ATP is 0.035 ± 0.009 mM, and the V_{max} is 0.0006% that observed for glycerol. The agreement between this apparent K_m and K_{ia} from the initial-velocity studies strongly suggests both the MgATPase and normal catalytic activity occur at the same site. Interestingly,

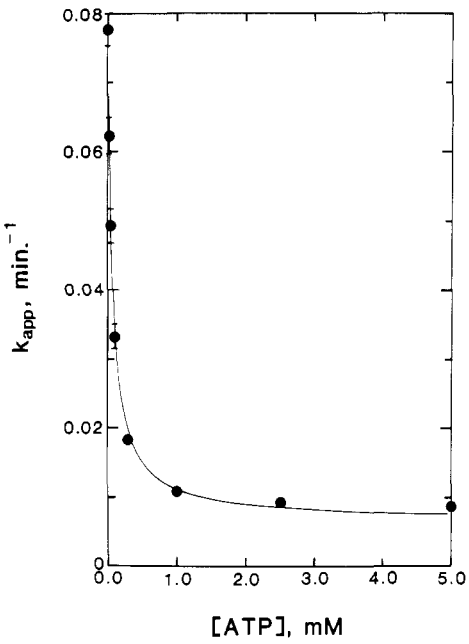

FIGURE 3: ATP dependence of the apparent rate constant for inactivation of glycerol kinase by NEM. The *points* are the rate constants obtained from the fits of the inactivation data to eq 5, and the *line* is the fit to eq 6 with the following parameter values: $k_e = 0.079 \pm 0.002$ min^{-1}, $k_{el} = 0.0067 \pm 0.0016$ min^{-1}, and $K_L = 0.067 \pm 0.011$ mM.

the double-reciprocal plots obtained in these experiments are linear to ATP concentrations of 5 mM, indicating the absence of the apparent substrate activation observed above.

Substrate Binding Studies. Affinities for substrate binding were determined by using protection from inactivation by NEM. The enzyme is inactivated by NEM in a reaction that obeys pseudo-first-order kinetics, and the rate of inactivation is decreased by substrate (Pettigrew, 1986). As described under Materials and Methods, an apparent dissociation constant for ligand binding can be estimated from the ligand concentration dependence of the inactivation kinetics. Representative data showing the dependence of the inactivation rate constant on ATP concentration at 10 mM $MgCl_2$ are presented in Figure 3. In all cases, the inactivation follows pseudo-first-order kinetics for at least three half-lives (data not shown). The *points* are the experimental data, and the *line* is the fit to eq 6. The data are well described by this mechanism, giving a reliable value for the dissociation constant.

Similar results are obtained for the other substrates. None of the tested substrates provided complete protection against inactivation; i.e., k_{el} was not zero for any substrate. Several explanations for this observation may be considered. It may indicate that the group(s) modified by NEM is not located at the substrate binding site(s). It may also indicate that the binding of the substrates to a second, lower affinity site alters the rate of inactivation by NEM; however, this possibility is eliminated by results of the binding stoichiometry experiments described below.

Dissociation constants, K_L, for binding of substrates estimated by using this method are listed in Table I. Experiments were performed in the absence of added Mg^{2+} and with 10 mM $MgCl_2$ added. The kinetics of the inactivation are not affected by the $MgCl_2$ alone, and the MgATPase rate is negligible at the enzyme concentrations used. The results show $MgCl_2$ has only small effects on the dissociation constants for the nucleotide substrates and glycerol-3P. In the cases of the nucleotides, this suggests there is little interaction between the enzyme and Mg^{2+} in the nucleotide complex. There is little difference in affinity for binding either of the nucleotide substrates, suggesting the γ-phosphate contributes little. Similarly, the phosphate group on glycerol-3P appears to contribute little to the binding affinity, since the affinities for glycerol and glycerol-3P are about the same.

The dissociation constants obtained from fitting the initial-velocity data at lower nucleotide concentrations, K_{iL}, are tabulated beside the constants obtained from the NEM protection method, K_L. Comparison of these values shows very good agreement between results obtained by using these independent methods. This indicates these ligands decrease the rate of inactivation by NEM by binding to the active site with the apparent higher affinity for nucleotides.

It is important to note the same affinity for ATP binding is obtained from these different experiments, which cover a range of protein concentrations from 0.2 μg/mL in the initial-velocity experiments to 0.05 mg/mL in the NEM protection experiments to 1 mg/mL in the MgATPase experiments, i.e., a 5000-fold range. Thus, the affinity for ATP binding does not depend on protein concentration over this range. Similarly, the same affinity for glycerol binding is obtained at 0.2 μg/mL in the initial-velocity studies and at 0.05 mg/mL in the NEM protection experiments, indicating no dependence of glycerol affinity on protein concentration over this 250-fold range.

Stoichiometry of Ligand Binding. While both the initial-velocity studies and the NEM inactivation protection studies could be interpreted in terms of more than one type of nucleotide binding site, neither of these studies provides direct information about the stoichiometry of substrate binding. Consequently, substrate binding stoichiometry was investigated by using equilibrium dialysis as described under Materials and Methods. The dissociation constant for ATP binding to the apparent lower affinity site estimated from the initial-velocity studies, K_{ia2}, is 0.23 ± 0.49 mM (Table I), and examination of Figure 2 suggests a similar affinity for ADP. This apparent low affinity of the putative second site for nucleotides requires the use of high concentrations of enzyme and ligand to detect binding. Consequently, enzyme concentrations of 0.3–1.0 mM (subunits), a glycerol concentration of 2 mM, and nucleotide concentrations of 1.9–2.1 mM were used to determine the stoichiometry of binding.

Stoichiometries of binding for ADP, ATP, and glycerol determined by equilibrium dialysis are shown in Table I. For these three ligands, the observed stoichiometry is consistent with half-of-the-sites binding. This observation is somewhat surprising. In the cases of the nucleotide substrates, binding at a regulatory site separate from the active site would be expected to give a stoichiometry greater than one. However, half-of-the-sites binding is observed for both nucleotides, as well as for glycerol, for which no regulatory kinetic behavior is observed. This result strongly suggests there is not a separate regulatory binding site for nucleotides and suggests a possible explanation for the kinetic behavior observed for the nucleotide substrates, which is discussed below.

The stoichiometry of binding of MgATP to phosphoglycerate kinase was determined as described under Materials and Methods. The average of two determinations was 1.6 mol of MgATP/mol of phosphoglycerate kinase, which agrees exactly with the reported value (Scopes, 1978). Thus, the dialysis method and methods of data analysis reliably detect multiple binding sites.

Discussion

Half-of-the-Sites Stoichiometry and Nucleotide Regulatory Properties. Both nucleotide substrates of *E. coli* glycerol

kinase show regulatory kinetic behavior. One possible explanation for this behavior is binding of the nucleotides to a regulatory site that is separate from the active site, such as observed in the cases of other kinases, including phosphoglycerate kinase (Scopes, 1978) and phosphofructokinase (Pettigrew & Frieden, 1979). However, two of the results obtained here strongly suggest this is not the case for *E. coli* glycerol kinase. First, the observation of a random kinetic mechanism for the enzyme shows that such a site does not have to be postulated to explain the formation of binary complexes with all substrates. Secondly, the half-of-the-sites stoichiometries observed for binding of the active-site ligands are not consistent with the presence of more than one ligand binding site per subunit and, as discussed below, provide a plausible explanation for the nucleotide regulation.

The half-of-the-sites stoichiometries observed for binding of these ligands to glycerol kinase do not appear to reflect problems with the dialysis method or methods of data analysis. These ligands have quite different chemical and physical properties, and different methods were used to determine their concentrations: radioactive glycerol was used, while absorbance spectroscopy was used for the nucleotides. The observation of the same stoichiometry of binding for these quite different substrates reduces the likelihood that the results are due to systematic error. Furthermore, the determinations of the stoichiometry of MgATP binding to phosphoglycerate kinase yield the value previously reported: 1.6 mol of MgATP/mol of phosphoglycerate kinase (Scopes, 1978).

Differences in the presence of Mg^{2+} and in the enzyme concentration in these experiments must be considered. No Mg^{2+} was present in the determinations of stoichiometry. However, the NEM protection experiments show that the affinity for binding of nucleotides is not dependent on Mg^{2+}. Enzyme concentrations in the equilibrium dialysis experiments were in the range of 25–58 mg/mL, which are 50-fold and 1100-fold greater than the highest concentrations used in determinations of the dissociation constants for nucleotides and glycerol, respectively. *E. coli* glycerol kinase undergoes a reversible polymerization reaction between dimers and tetramers (DeRiel & Paulus, 1978); at 0.05 mg/mL, its weight-average molecular size corresponds to that expected for the dimer.[4] The agreement between the dissociation constants estimated from the initial-velocity and NEM protection studies indicates the affinity for nucleotides and glycerol does not change over enzyme concentrations in the range from 0.2 μg/mL to 0.05 mg/mL, and the agreement of K_M for the MgATPase activity with the dissociation constants from the initial-velocity and NEM protection experiments further indicates the affinity for ATP is not dependent on enzyme concentration up to 1 mg/mL. The half-of-the-sites stoichiometry obtained for glycerol binding in these experiments agrees with a previous report in which the binding stoichiometry was determined at enzyme concentrations comparable to those of the NEM experiments (Thorner & Paulus, 1973).[5] These considerations suggest the half-of-the-sites stoichiometries observed here are not due to differences in the enzyme concentrations used in the different experiments.

The half-of-the-sites ligand binding stoichiometry is consistent with one possible explanation for the apparent regulatory behavior observed for the nucleotide substrates. At the protein concentrations used in the initial-velocity studies, the dimer is presumably the predominant enzyme form present. While the molecular size of the enzyme under the conditions of the initial-velocity studies has not been demonstrated analytically, there are no physical–chemical data that show or suggest monomeric enzyme forms at these low concentrations. Both the half-of-the-sites stoichiometry of substrate binding and the apparent regulatory behavior seen with the nucleotide substrates are consistent with models in which the minimal size of the enzyme in the assay is the dimer and the subunits of the dimer display markedly different affinities for binding substrates. Two limiting cases of such models may be considered. In one case, the dimer exhibits intrinsic asymmetry and has two classes of binding sites with different affinities for substrates. In the other case, binding of substrate to one subunit of a symmetrical dimer results in a large decrease in the affinity of the other subunit for substrate binding, i.e., negative cooperativity between the binding sites.

Discrimination between these cases is difficult. However, several of the observed properties of the enzyme are consistent with interactions between nucleotides binding to the active sites on different subunits of the dimer. In the absence of a separate regulatory site, the substrate inhibition by ADP is consistent with cooperativity in nucleotide binding to different subunits and is difficult to explain in terms of two classes of noninteracting binding sites. Interactions between bound substrates in the ternary complexes, which is one possible explanation for the difference between the Michaelis and dissociation constants, suggest conformational changes that could be involved in communication between active sites. A possible role for interactions in the ternary complexes is further indicated by the observation that apparent second binding sites are seen for the nucleotides in the kinetics experiments while the stoichiometry determinations, performed on the binary complexes, provide no indication of the second site. This suggests that formation of the ternary complex at one nucleotide binding site, with consequent conformational changes, is required for binding at the second site; i.e., formation of binary complexes is not sufficient for binding of either substrate at the second site. This observation is difficult to reconcile in the context of an asymmetric dimer, in which case binding to the lower affinity site would be expected to be observed at the higher ligand concentrations used in these experiments. Finally, the failure of high concentrations of any ligand to provide complete protection of the enzyme from inactivation by NEM is consistent with the case in which occupancy of one active site of the dimer upon formation of the binary complex leaves the second active site available for modification. The decreased rate of inactivation of the binary complex suggests that conformational changes do occur upon formation of the binary complexes. In the case of glycerol, formation of the binary complex can be observed by difference spectroscopy, which is consistent with a conformational change.[4]

Other explanations for the curvature in the double-reciprocal plots of Figures 1 and 2 can be considered. The curvature may result from a difference in the rates of the two pathways of substrate addition and product release in a random kinetic mechanism in which the rapid equilibrium assumption does not hold. This case predicts two kinetic behaviors that are not

[4] D. W. Pettigrew, unpublished observations.

[5] In the previous report, glycerol stoichiometries of 0.25–0.5 mol of glycerol/mol of enzyme (subunit) were determined by an ultrafiltration method. Those authors postulated that the low stoichiometry was due to inactivation of the enzyme during preparatory dialysis in the absence of glycerol. Using the method of Hummel and Dreyer, they obtained a stoichiometry for glycerol binding of about 1 mol/mol of enzyme (subunit). In these latter experiments, ADP was present in the column buffers. In our equilibrium dialysis experiments, ADP does not alter the stoichiometry of glycerol binding (D. W. Pettigrew and Y. Liu, unpublished experiments). Our attempts to reproduce the Hummel–Dreyer experiments have not been successful.

observed for *E. coli* glycerol kinase. First, nonlinear double-reciprocal plots should be observed for both substrates in a given reaction direction (Segel, 1975). For *E. coli* glycerol kinase, only linear double-reciprocal plots are observed for glycerol or glycerol-3P. Secondly, the nonlinear double-reciprocal plots should become linear at saturating concentrations of the other substrate (Pettersson, 1969); for *E. coli* glycerol kinase, the plots are nonlinear at all concentrations of glycerol and glycerol-3P that have been examined.

The nonlinear double-reciprocal plots observed for ATP and ADP may result from their binding to the enzyme/glycerol-3P and enzyme/glycerol complexes, respectively, in the context of a kinetic mechanism in which product release is at least partially rate-limiting. The substrate activation by ATP could be due to its increasing the rate of glycerol-3P dissociation, while ADP inhibition could be due to its decreasing the rate of glycerol dissociation. Results of the enzyme kinetics studies indicate that if the nucleotides do bind to the respective binary complexes, the binding occurs either at a second site different from the apparent higher affinity site or in a different mode of binding at that site. The product inhibition studies show the enzyme/glycerol-3P/MgATP complex does not form at the higher affinity nucleotide binding site. The initial-velocity studies show the dissociation constant for nucleotide binding that results in regulatory behavior is in the range of 0.5 mM. The product inhibition studies show that the enzyme/glycerol/MgADP complex forms; but there appears to be no interactions between these bound substrates, and the dissociation constant for MgADP binding to this complex should be 0.14 mM. As discussed above, the binding stoichiometries provide no evidence for a regulatory binding site that is different from the active site.

Possible Physiological Significance. The apparent nucleotide regulatory properties of *E. coli* glycerol kinase are consistent with its physiological role as the catalyst of the rate-limiting step in glycerol utilization (Zwaig et al., 1970). In the forward reaction direction, the Michaelis constants for both substrates are 10-fold less than the dissociation constants and are in the low micromolar range. As a consequence, the efficiency of the enzyme is quite high. Examination of Table I shows the values of k_{cat}/K_m for both substrates in the forward reaction direction approach the diffusion-controlled limit.

The high efficiency of glycerol kinase may be important because of the important roles played by the product of the reaction, glycerol-3P. The components of the pathway for glycerol metabolism in *E. coli* are coded for by the elements of the *glp* regulon (Lin, 1976). The inducer for regulon expression is glycerol-3P, the product of the glycerol kinase reaction. Because of the high efficiency of glycerol kinase, even the low, uninduced level of the enzyme can produce significant amounts of the inducer when the cell is in an environment with a high glycerol concentration. Because the uninduced level of the aerobic glycerol-3P dehydrogenase is quite low, the concentration of glycerol-3P could then rapidly rise, resulting in induction of the regulon elements. Considered in this context, the apparent activation by ATP is not paradoxical. The significant aspect of this behavior occurs at low nucleotide concentrations rather than at higher nucleotide concentrations where apparent activation, in terms of increased V_{max}, is observed. The regulatory properties of glycerol kinase appear to be finely tuned to function as a sensor of conditions related to glycerol metabolism, communicating information to the genes that produce the enzymes. Thus, its nucleotide regulatory properties allow it to efficiently produce the inducer when glycerol is available, and its regulation by fructose 1,6-bisphosphate allows the rapid shutdown of inducer synthesis if sugars become available.

The *glp* regulon appears to be unique in terms of this type of regulation in *E. coli*. There are few inducible metabolic systems in *E. coli* for which the inducer is a metabolite of the molecule; these include the *lac* operon, the *fuc* regulon, and sucrose metabolism (Ingraham et al., 1987). In these cases, none of the enzymes that have been examined show regulatory behavior.

Kinetic Mechanism of E. coli Glycerol Kinase. The results of the dead-end and product inhibition studies described above are consistent with a random kinetic mechanism for *E. coli* glycerol kinase. This conclusion is supported by the observation of formation of the binary complexes with all the substrates and by the MgATPase activity of the enzyme. Binding of the ligands to the active site of the enzyme in formation of the binary complexes is supported by the agreement between the dissociation constants obtained from the initial-velocity and NEM protection experiments.

At the time these studies were undertaken, previous investigations had reported an ordered kinetic mechanism for both *E. coli* (Thorner & Paulus, 1973) and *Candida mycoderma* (Janson & Cleland, 1974) glycerol kinases. In the case of the *E. coli* enzyme, the formation of binary complexes with high affinity for all the substrates cast doubt on the ordered kinetic mechanism. Recently, the kinetic mechanism of the glycerol kinase from *C. mycoderma* has been reinvestigated and a random mechanism has been concluded to be the case for this enzyme (Knight & Cleland, 1989). Thus, both glycerol kinases that have been characterized appear to have a random kinetic mechanism.

Acknowledgments

The technical assistance of Ms. Sandra Scarborough is gratefully acknowledged. Some of the ligand dissociation constants were determined by Brian Beck, and the MgATPase studies were performed by Daryll DeWald. The figures were expertly prepared by Lisa Lohman. We thank Dr. Al Mildvan for bringing the paper of Scrutton and Utter to our attention and Dr. Paul Fitzpatrick for helpful discussions.

References

DeRiel, Jon K., & Paulus, Henry (1978) *Biochemistry 17*, 5141–5146.

Faber, H. R., Pettigrew, D. W., & Remington, S. J. (1989) *J. Mol. Biol. 207*, 637–639.

Ingraham, J. L., Brookslow, K., Magasanik, B., Schoechter, M., & Umbargar, H. E., Eds. (1987) *Escherichia coli and Salmonella typhimurium, Cellular & Molecular Biology*, American Society for Microbiology, Washington, DC.

Knight, W. B., & Cleland, W. W. (1989) *Biochemistry 28*, 5728–5734.

Lin, E. C. C. (1976) *Annu. Rev. Microbiol. 30*, 535–578.

Pettersson, G. (1969) *Acta Chem. Scand. 23*, 2717–2726.

Pettigrew, Donald W., & Frieden, C. (1979) *J. Biol. Chem. 254*, 1887–1895.

Pettigrew, Donald W. (1986) *Biochemistry 25*, 4711–4717.

Pettigrew, Donald W. (1987) *Biochemistry 26*, 1723–1727.

Pettigrew, Donald W., Ma, Din-Pow, Conrad, Charles A., & Johnson, James R. (1988) *J. Biol. Chem. 263*, 135–139.

Scopes, Robert K. (1978) *Eur. J. Biochem. 91*, 119–129.

Scrutton, Michael C., & Utter, Merton F. (1965) *J. Biol. Chem. 240*, 3714–3723.

Segel, I. H. (1975) *Enzyme Kinetics*, p 460, John Wiley & Sons, New York.

Thorner, Jeremy W., & Paulus, Henry (1971) *J. Biol. Chem. 246*, 3885–3894.
Thorner, Jeremy W., & Paulus, Henry (1973) *J. Biol. Chem. 248*, 3922–3932.
Turner, B. W., Pettigrew, D. W., & Ackers, G. K. (1981) *Methods Enzymol. 76*, 586–629.
Zwaig, N., & Lin, E. C. C. (1966) *Science 153*, 755–757.
Zwaig, N., & Lin, E. C. C. (1970) *J. Bacteriol. 102*, 753–759.

Role of the Zinc(II) Ions in the Structure of the Three-Finger DNA Binding Domain of the Sp1 Transcription Factor†

Jun Kuwahara‡ and Joseph E. Coleman*
Department of Molecular Biophysics and Biochemistry, Yale University, New Haven, Connecticut 06510
Received April 23, 1990; Revised Manuscript Received June 6, 1990

ABSTRACT: The transcription factor Sp1 from Hela cells contains near the C-terminus of this protein of 778 amino acids three contiguous repeats of an amino acid sequence, -Cys-X_4-Cys-X_{12}-His-X_3-His-, typical of the Cys_2His_2-type zinc-finger DNA binding domain first found in transcription factor TFIIIA. A DNA sequence corresponding to the codons from residue 614 to residue 778 of Sp1 (encompassing the three zinc-finger motifs) has been cloned and overproduced in *Escherichia coli*. The fragment of Sp1 containing the C-terminal 165 residues plus 2 from the cloning vector, designated Sp1(167*), can be extracted with 5 M urea and then refolded in the presence of Zn(II) to a protein of specific conformation containing 3.0 ± 0.2 mol of tightly bound Zn(II)/mol of protein. Gel retardation assays using a labeled 14-bp DNA sequence containing a consensus Sp1 binding site show that the refolded Zn(II) protein specifically recognizes the "GC box" sequence in the presence of a large excess of calf thymus DNA. Treatment of Zn(II)Sp1(167*) with 10 mM EDTA results in removal of Zn(II) and the formation of an apoprotein which does not specifically recognize DNA. Cd(II) can be exchanged for Zn(II) in the refolded protein with full retention of specific DNA recognition. This is the first Cys_2His_2-type "finger" protein where this substitution has been accomplished. Titration of the Zn(II) protein with 6 mol of *p*-mercuribenzenesulfonate/mol of protein results in the complete release of the three Zn(II) ions. Release of Zn(II) is highly cooperative. Reaction of only two of the sulfhydryl zinc ligands with the organic mercurial releases 75% of the Zn(II), suggesting that the Zn(II)-induced folding of the three fingers is probably cooperative. Circular dichroism shows the $Zn(II)_3$ protein to contain ~20% α-helix, ~20% β-sheet, and ~60% random coil as the secondary structure of the zinc-finger domain. A large part of the secondary structure is lost when the metal ions are removed.

Transcription factor Sp1 is a protein of 105 kDa containing 778 amino acids which activates a reasonably large subset of mammalian genes containing "GC box" upstream promoter elements (Dynan & Tjian, 1985; Kadonaga et al., 1986, 1987; McKnight & Tjian, 1986; Courey et al., 1989). The C-terminal 168 amino acid residues of Sp1 contain three contiguous zinc-finger motifs, -Cys-X_4-Cys-X_{12}-His-X_3-His-, which are believed to bind Zn(II). The C-terminal domain has been shown to constitute the DNA binding domain, while the N-terminal 610 amino acid residues form the trans activating domain. Structural features of the latter include two distinct glutamine-rich regions (Courey et al., 1989). Deletion mutations and domain swapping experiments on Sp1 show that the two domains function independently (Courey & Tjian, 1988; Courey et al., 1989). In order to study the structure and metal ion binding properties of the DNA binding domain of Sp1, the C-terminal 165 amino acids were cloned into an overproduction vector under the control of a T7 RNA polymerase promoter. While expressed in high yield, the 165-residue construct is insoluble as expressed in *Escherichia coli* but can be resolubilized and refolded after extraction with 5 M urea. Attempts to solubilize the finger domain of Sp1 by fusing it to the highly soluble C-terminal domain of glutathione-*S*-transferase resulted in an insoluble fusion protein. Refolding of the 165 amino acid fragment in the presence of metal ions, however, results in a protein that contains three Zn(II) ions in a stable secondary structure which specifically recognizes the GC box of the Sp1 binding site. The properties of that protein are described in this paper.

Materials and Methods

Cloning of the DNA Binding Subdomain of Sp1. The plasmid Sp1-1 coding for the C-terminal 696 amino acids of transcription factor Sp1 was kindly supplied by James Kadonaga and Robert Tjian of the University of California, Berkeley. A number of different fragments from the C-terminal region of Sp1 containing the three zinc-finger sequences were cloned into pAR3039 plasmid under the control of a T7 promoter and the products overexpressed in the host *E. coli* BL21(DE3), which carries a chromosomal copy of the T7 gene 1 under the control of the lac promoter and is subject to induction by IPTG (Studier & Moffatt, 1986). The constructs are listed below as Sp1($x + y$), where x refers to the number of codons from the Sp1 gene while y indicates the number of extra codons from the cloning vector. The following constructs resulted in overexpressed products: Sp1(167 + 12) containing residues 612–778 of Sp1 and obtained from a *Bam*H1/*Hin*dIII fragment of the Sp1 gene with an additional 12 residues from T7 gene 10 contributed from the cloning vector at the N-

† This work was supported by NIH Grants DK09070 and GM21919.
* Corresponding author.
‡ Present address: Institute for Chemical Research, Kyoto University, Uji, Kyoto 611, Japan.

0006-2960/90/0429-8627$02.50/0 © 1990 American Chemical Society